Infrared spectra and structures of $(CH_3NH_2)_nH^+$ (n = 1–4).   Binding features of an excess proton

Takayuki Michi [a], **Kazuhiko Ohashi** [b,*], **Yoshiya Inokuchi** [c],

Nobuyuki Nishi [c], **Hiroshi Sekiya** [b]

[a] *Department of Chemistry, School of Sciences, Kyushu University,*

Hakozaki, Fukuoka 812-8581, Japan

[b] *Department of Chemistry, Faculty of Sciences, Kyushu University,*

Hakozaki, Fukuoka 812-8581, Japan

[c] *Institute for Molecular Science, Myodaiji, Okazaki 444-8585, Japan*

Abstract

Infrared photodissociation spectra of $CH_3NH_3^+$–Ar and $(CH_3NH_2)_nH^+$ with n = 2–4 are measured in the 2600–3500 cm^{-1} region and analyzed with the aid of ab initio calculations. The intensities of the CH-stretching transitions relative to the NH-stretching transitions increase with increasing n, suggesting the change of the binding features of an excess proton in the clusters.   Two CH_3NH_2 molecules in $(CH_3NH_2)_2H^+$ equally share the proton.   On the other hand, the proton is localized on the central molecule in $(CH_3NH_2)_4H^+$, forming the $CH_3NH_3^+$ core solvated by three CH_3NH_2 molecules.

_____

[*] Corresponding author.   Fax: +81-92-642-2607.

E-mail address: kazu.scc@mbox.nc.kyushu-u.ac.jp   (K. Ohashi).

1. Introduction

Proton transfer is a common and essential reaction in various chemical and biological systems [1]. Specifically, the proton transport process in liquid water has been the focus of interest because of anomalously large mobility of proton [2]. An explanation for the large mobility invokes periodic interconversion between H_3O^+-centered and $H_5O_2^+$-centered clusters [3]. The efficiency of the interconversion may sensitively depend on the number and arrangement of molecules surrounding the central ions. In regard to this, $H^+(H_2O)_n$ and related species have been investigated in the gas phase for elucidating the properties of the proton solvation and transport in liquid phase from a microscopic point of view. Lee and co-workers have introduced the vibrational predissociation spectroscopy to investigate the structures of $H^+(H_2O)_n$ [4,5]. In the analysis of the vibrational spectra, they assume that the structure of $H^+(H_2O)_2$ is symmetric with respect to the position of the proton between two H_2O molecules [6,7]. High-level ab initio calculations support this assumption, predicting that the equilibrium geometry of $H^+(H_2O)_2$ corresponds to the symmetric $H_2O–H^+–OH_2$ structure [8]. On the other hand, the spectra of $H^+(H_2O)_3$ and $H^+(H_2O)_4$ are compatible with H_3O^+-centered structures of the form $H_3O^+\cdots(H_2O)_{2,3}$, where the proton is localized on the central molecule. For $H^+(H_2O)_n$ with $n = 6–8$, systematic comparison of the experimental and theoretically calculated spectra provides evidence for the coexistence of the $H_3O^+\cdots(H_2O)_{n–1}$ and $H_5O_2^+\cdots(H_2O)_{n–2}$ isomers [5].

The questions associated with the structures of $(NH_3)_nH^+$ are analogous to those discussed for $H^+(H_2O)_n$. In contrast to $H^+(H_2O)_2$, most of ab initio calculations for $(NH_3)_2H^+$ suggest that the symmetric $H_3N–H^+–NH_3$ structure is less stable than the asymmetric $NH_4^+–NH_3$ structure, where the proton is localized on one NH_3 molecule [9]. However, the analysis and simulation of the vibrational spectrum indicate that the symmetric structure is consistent with the experimental observations [10]. Further investigations are required to resolve the inconsistency between the experiment and theory. For $(NH_3)_nH^+$ with $n > 2$, the vibrational spectra provide information on the solvation structures [10,11]. The first four NH_3 molecules form hydrogen bonds to the four protons of the central NH_4^+

ion.   Filling up of the first solvation shell at $NH_4^+ \cdots (NH_3)_4$ is also supported by ab initio calculations [9,11] and mass spectrometric studies [12].

In the present work, we direct our attention to the protonated methylamine clusters, $(CH_3NH_2)_nH^+$.   The replacement of a hydrogen atom of NH_3 by a methyl group results in the following spectral character of the molecule.   Theoretical calculations of the infrared spectra for the bare and protonated CH_3NH_2 predict that the relative intensities of the CH-stretching and NH-stretching transitions change considerably upon the attachment of the proton [13].   This characteristic feature will provide a method of probing the position of the proton between a pair of CH_3NH_2 molecules in the clusters.   Thus, we measure the infrared spectra of $(CH_3NH_2)_nH^+$ by the photodissociation spectroscopy.   The experimental results are analyzed with the aid of density functional theory (DFT) calculations.

2. Experimental and Computational

Infrared photodissociation spectra of $(CH_3NH_3)^+-Ar$ and $(CH_3NH_2)_nH^+$ ($n = 2$–4) are measured by using a triple quadrupole mass spectrometer [14].   The protonated methylamine clusters are produced in an ion source of electron-impact type.   The parent ions of interest are isolated by the first quadrupole mass filter.   After deflection by an ion bender, the ions are introduced into the second quadrupole ion guide and irradiated by an infrared laser (Continuum, Mirage 3000).   The vibrational excitation induces predissociation of the parent ions.   After leaving the ion guide, the fragment ions are analyzed by the third quadrupole mass spectrometer.   The photodissociation spectra are taken by recording the yields of the fragment ions as a function of wavenumber of the infrared laser.

Theoretical calculations are carried out with Gaussian 98 program package [15].   The geometries of CH_3NH_2, $CH_3NH_3^+$ and $(CH_3NH_2)_nH^+$ ($n = 2$–4) are optimized using the hybrid DFT method (B3LYP) with double zeta Dunning's correlation consistent basis sets (cc-pVDZ).   The harmonic vibrational frequencies and infrared absorption intensities are evaluated for comparing the theoretical infrared spectra with the observed ones.   A factor of 0.9635 is used to scale the frequencies of all the vibrations of all the species.

3. Results and discussion

3.1. Optimized structures

Fig. 1 illustrates the structures of $(CH_3NH_2)_nH^+$ ($n = 2\text{--}4$) obtained by DFT calculations. An excess proton in $(CH_3NH_2)_2H^+$ is located between the N atoms of CH_3NH_2 molecules. One of the aims of the present study is to determine the position of the proton in further detail. Figs. 1a and b show two different structures of $(CH_3NH_2)_2H^+$ in regard to the position of the proton, which belong to the C_1 and C_2 symmetry, respectively. In the C_1 structure (Fig. 1a), the proton is located close to one of the two N atoms. In the C_2 structure (Fig. 1b), on the other hand, the proton is situated in the middle of the two N atoms. DFT calculations predict that the C_1 structure is located at the potential energy minimum and that the C_2 structure is a transition state of proton transfer between the two CH_3NH_2 molecules.

Figs. 1c and d depict the minimum-energy structures of $(CH_3NH_2)_3H^+$ and $(CH_3NH_2)_4H^+$, respectively. In these structures, the proton is attached to the N atom of the central molecule, forming a $CH_3NH_3^+$ subunit. The central $CH_3NH_3^+$ ion provides a maximum of three hydrogen-bonding sites for the surrounding molecules. In $(CH_3NH_2)_3H^+$ (Fig. 1c), two CH_3NH_2 molecules are bound to two of the three sites through an N–H···N hydrogen bond. In $(CH_3NH_2)_4H^+$ (Fig. 1d), the central $CH_3NH_3^+$ ion forms hydrogen bonds with three CH_3NH_2 molecules in the first solvation shell. Tzeng et al. predicted a similar structure from ab initio calculations at the HF/6-31G** level [16]. They proposed that the complete filling of hydrogen-bonding sites on the central ion is responsible for anomalous stability of $(CH_3NH_2)_4H^+$ observed as a magic number in the mass spectrum of $(CH_3NH_2)_nH^+$. One may expect an isomeric structure of $(CH_3NH_2)_4H^+$ with two CH_3NH_2 molecules in the first solvation shell and one CH_3NH_2 in the second shell. However, the structure with completely filled first shell is considered to be the most stable one, as demonstrated by ab initio calculations for $NH_4^+(NH_3)_4$ [9].

3.2. CH_3NH_2 and $CH_3NH_3^+$

4

Figs. 2a and b display theoretical infrared spectra of CH_3NH_2 and $CH_3NH_3^+$, respectively. The vibrations of CH_3NH_2 with significant absorption intensities in this region are the CH-stretching modes located at 2837, 2941 and 2980 cm^{-1}. The NH stretching modes at 3327 and 3395 cm^{-1} have much lower intensities. The attachment of a proton to CH_3NH_2 drastically changes the spectral features. The CH-stretching transitions of $CH_3NH_3^+$ at 2973 and 3082 cm^{-1} become extremely weak and the prominent vibrations switch to the NH-stretching modes. The transitions at 3258 and 3336 cm^{-1} are due to the symmetric and degenerate antisymmetric stretching vibrations of the NH_3 group, respectively. The results of the present DFT calculations are in good agreement with those of MP2/6-311G** calculations reported by Zeroka and Jensen [13].

The experimental infrared spectrum of CH_3NH_2 vapor in the literature [17] is consistent with the theoretical spectrum (Fig. 2a). On the other hand, the infrared and Raman data of $CH_3NH_3^+$ are available only for crystalline methylammonium halides [18,19], where $CH_3NH_3^+$ is subject to strong perturbations by adjacent halogen anions. Therefore, we need to obtain the spectrum of the isolated $CH_3NH_3^+$ for verifying the prediction from theoretical calculations. Here we measure the spectrum of $CH_3NH_3^+$–Ar instead of $CH_3NH_3^+$, because the infrared photodissociation spectroscopy is applicable only to the species that undergo predissociation subsequent to the vibrational excitation. From our preliminary calculations, we confirm that the attachment of Ar to $CH_3NH_3^+$ hardly changes the relative intensities of the CH and NH bands. Fig. 2c exhibits the photodissociation spectrum of $CH_3NH_3^+$–Ar. A prominent band is observed at 3325 cm^{-1} with a weaker one at 3270 cm^{-1} in the region of the NH-stretching vibrations. The absorption intensities in the CH-stretching region are negligibly small. The theoretical spectrum of $CH_3NH_3^+$ (Fig. 2b) reasonably reproduces the relative intensities of the CH and NH bands observed in the experimental spectrum of $CH_3NH_3^+$–Ar (Fig. 2c).

3.3. $(CH_3NH_2)_2H^+$

The considerable difference in the spectral features between the bare and protonated methylamine molecules provides a method of probing the binding features of an excess

proton in the clusters.   Fig. 3a represents the photodissociation spectrum of $(CH_3NH_2)_2H^+$. The absorption bands in the CH-stretching region become recognizable but their intensities are still one order of magnitude weaker than those of the NH-stretching bands.   From the weakness of the CH bands, one may infer the C_2 structure for $(CH_3NH_2)_2H^+$, where both CH_3NH_2 molecules are under the influence of the proton.   The theoretical spectrum calculated by assuming the C_2 structure is shown in Fig. 3b.   The transitions at 3310 and 3371 cm^{-1} are due to out-of-phase combinations of the symmetric and antisymmetric stretching vibrations, respectively, of the NH_2 group of each CH_3NH_2 subunit.   The reduced intensities of the CH bands in the theoretical spectrum (Fig. 3b) are in good agreement with those observed in the experimental spectrum (Fig. 3a).   However, the intensities of the CH bands are also weak in the spectrum calculated by assuming the C_1 structure (Fig. 3c), although one CH_3NH_2 molecule is located at a distance from the proton.   Contrary to the expectation based on the spectra of CH_3NH_2 and $CH_3NH_3^+$, the theoretical spectra for the C_1 and C_2 structures are quite similar to each other so that the two structures cannot be discriminated by the infrared spectroscopy.

Yin and Green extensively carried out ab initio calculations (at the B3LYP/D95^{+*} and MP2/6-31+G* levels of theory) of $(CH_3NH_2)_2H^+$ for determining the potential energy surface (PES) composed of thousands of points [20].   Our DFT calculations are performed only for the geometries corresponding to stationary points on the PES.   The C_1 structure obtained from our calculations is in good agreement with the one optimized by Yin and Green.   They also obtained the wave function of the proton by using a three-dimensional form of the Fourier grid Hamiltonian technique.   The PES has two minima corresponding to the C_1 structure.   However, the barrier between the minima is so small that the PES appears to have a single well.   As a result, the calculated wave function of the proton exhibits the maximum in the middle of the two N atoms, which essentially corresponds to the C_2 structure. Therefore, we believe that $(CH_3NH_2)_2H^+$ takes the C_2 structure on account of the quantum effect, although the potential energy minima exist at the C_1 structure.

As for $(NH_3)_2H^+$, the situation is analogous to that described above for $(CH_3NH_2)_2H^+$. Recently, Asada and co-workers studied the proton transfer in $(NH_3)_2H^+$ by using a one-

dimensional model for the quantum wave packet dynamics on the ab initio MP2/6-31+G* PES [21]. The optimization yields the asymmetric NH_4^+–NH_3 structure, where the proton is bound to one NH_3 molecule. However, a flat shape of the PES causes the proton to be situated in the middle of the two NH_3 molecules, which corresponds to the symmetric H_3N–H^+–NH_3 structure. Due to the quantum nature of the proton, the experimental results of $(NH_3)_2H^+$ reported by Price et al. [10], and of $(CH_3NH_2)_2H^+$ obtained in this work, are consistent with the structure where the proton is equally shared between the two molecules.

3.4. $(CH_3NH_2)_3H^+$ and $(CH_3NH_2)_4H^+$

Fig. 4a exhibits the experimental infrared spectrum of $(CH_3NH_2)_3H^+$. The CH-stretching transitions show appreciable intensities compared to those of $(CH_3NH_2)_2H^+$. The emergence of the CH bands suggests that at least one CH_3NH_2 molecule in $(CH_3NH_2)_3H^+$ is located at a distance from the proton. The structure obtained from our DFT calculations is consistent with this suggestion. In the minimum-energy structure of $(CH_3NH_2)_3H^+$ (Fig. 1c), the proton is attached to the N atom of the central molecule, forming the $CH_3NH_3^+$ core. Two CH_3NH_2 molecules are bound to two of the three hydrogen-bonding sites of the $CH_3NH_3^+$ core through an N–H$\cdots$N hydrogen bond. The H$\cdots$N distance in each hydrogen bond is 1.596 Å. The corresponding distance in the C_1 structure of $(CH_3NH_2)_2H^+$ (Fig. 1a) is 1.564 Å. Concerning the minimum-energy structure, the H$\cdots$N distance lengthens slightly on going from $(CH_3NH_2)_2H^+$ to $(CH_3NH_2)_3H^+$. The intensities of the CH and NH bands calculated for the minimum-energy structure are comparable with each other. The theoretical infrared spectrum (Fig. 4b) coincides well with the experimental spectrum (Fig. 4a).

The spectral features assigned to the CH stretching transitions are extremely broad and the intensities are still appreciable in the 2600–2900 cm^{-1} region, where no fundamental transitions are seen in the theoretical spectrum. The appearance of overtone transitions through Fermi resonance interaction may be responsible for the broad features, because overtone bands of NH and CH bending vibrations are expected to appear in this region. The

experiment using partially deuterated isotopomers of methylamine may be helpful in elucidating the origin of the broadness.

Fig. 4c shows the experimental spectrum of $(CH_3NH_2)_4H^+$. The CH bands predominate over the NH bands; the spectrum approaches that of CH_3NH_2. These spectral features suggest that most of CH_3NH_2 molecules in the cluster are free from the influence of the proton. In the minimum-energy structure of $(CH_3NH_2)_4H^+$ (Fig. 1d), three CH_3NH_2 molecules are bound to the $CH_3NH_3^+$ core through an N–H$\cdots$N hydrogen bond. The H$\cdots$N distance in each hydrogen bond increases further to 1.754 Å, suggesting the localization of the proton on the central molecule. From DFT calculations, the integrated intensity of the CH bands is larger than that of the NH bands by a factor of approximately 7. The theoretical spectrum (Fig. 4d) calculated for the minimum-energy structure holds an excellent fit to the experimental spectrum (Fig. 4c).

Yin and Green examined the PES of $(CH_3NH_2)_2H^+$ as a function of the distance between the N atoms [20]. The geometry optimization without any constraint results in the N$\cdots$N distance of 2.71 Å. As described in section 3.3, the proton can be delocalized between the N atoms due to the extremely low barrier on the PES. If the N$\cdots$N distance is intentionally constrained to 3.2 or 3.6 Å, however, then the barrier becomes sufficiently high. As a result, the calculated wave function of the proton exhibits the maximum at one of the two potential energy minima. The N$\cdots$N distance is regarded as one of the most important parameter in determining whether the proton is localized or not. From our DFT calculations, the N$\cdots$N distance is found to increase from 2.63 Å in $(CH_3NH_2)_3H^+$ to 2.81 Å in $(CH_3NH_2)_4H^+$. This implies that the potential barrier becomes higher with increasing the cluster size. In larger clusters, therefore, the proton is forced to spend most of its time close to the N atom of the central molecule; the other molecules are almost free from the influence of the proton. The CH-stretching transitions become increasingly strong relative to the NH-stretching transitions with increasing the cluster size. The size-dependent change of the infrared spectra is totally consistent with the change of the binding features of the proton in $(CH_3NH_2)_nH^+$.

4. Conclusions

The vibrations of $CH_3NH_3^+$ with substantial absorption intensities are the NH-stretching modes, in striking contrast to CH_3NH_2 with significant intensities of the CH-stretching modes.   The relative intensities of the CH and NH bands sensitively change upon the attachment of the proton.   We have taken advantage of these characteristic features to investigate the binding features of the proton in $(CH_3NH_2)_nH^+$.   The measurement of the infrared spectra of $(CH_3NH_2)_nH^+$ reveals that the intensities of the CH bands increase gradually while those of the NH bands decrease with increasing the cluster size.   These results suggest the change of the probability distribution of the proton between a pair of N atoms of CH_3NH_2 molecules in the clusters.   The experimental spectrum of $(CH_3NH_2)_2H^+$ is consistent with the theoretical prediction that the proton is equally shared between two N atoms.   On the other hand, the proton is localized on the N atom of the central molecule in $(CH_3NH_2)_3H^+$ and the localization is prominent in $(CH_3NH_2)_4H^+$.

References

[1]   H. H. Limbach,   J. Manz,   Ber. Bensenges. Phys. Chem.   102   (1998) 289.

[2]   N. Agmon,   Isr. J. Chem.   39   (1999)   493.

[3]   M. Tuckerman,   K. Laasonen,   M. Sprik,   M. Parrinello,   J. Chem. Phys. 103   (1995)   150.

[4]   M. W. Crofton,   J. M. Price,   Y. T. Lee,   in: H. Haberland   (Ed.), Clusters of Atoms and Molecules II,   Springer, Berlin, 1994,   p. 44.

[5]   J.-C. Jiang,   Y.-S. Wang,   H.-C. Chang,   S.-H. Lin,   Y. T. Lee,   G. Niedner-Schatteburg,   H.-C. Chang,   J. Am. Chem. Soc.   122   (2000)   1398.

[6]   L. I. Yeh,   M. Okumura,   J. D. Myers,   J. M. Price,   Y. T. Lee,   J. Chem. Phys.   91   (1989)   7319.

[7]   M. Okumura,   L. I. Yeh,   J. D. Myers,   Y. T. Lee,   J. Phys. Chem.   94 (1990)   3416.

[8]   E. F. Valeev,   H. F. Schaefer, III,   J. Chem. Phys.   108   (1998)   7197.

[9]   B.-C. Wang,   J.-C. Chang,   J.-C. Jiang,   S.-H. Lin,   Chem. Phys.   276 (2002)   93.

[10]   J. M. Price,   M. W. Crofton,   Y. T. Lee,   J. Phys. Chem.   95   (1991) 2182.

[11]   M. Ichihashi,   J. Yamabe,   K. Murai,   S. Nonose,   K. Hirao,   T. Kondow, J. Phys. Chem.   100   (1996)   10050.

[12]   A. W. Castleman, Jr,   W. B. Tzeng,   S. Wei,   S. Morgan,   J. Chem. Soc. Faraday Trans.   86   (1990)   2417.

[13]   D. Zeroka,   J. O. Jensen,   J. Mol. Struct. (Theochem)   425   (1998)   181.

[14]   Y. Inokuchi,   N. Nishi,   J. Chem. Phys.   114   (2001)   7059.

[15]   M. J. Frisch   et al.,   Gaussian, Inc.,   Pittsburgh PA,   1998.

[16]   W. B. Tzeng,   K. Narayanan,   G. C. Chang,   W. C. Tsai,   J. J. Ho,   J. Phys. Chem.   100   (1996)   15340.

[17]   A. P. Gray,   R. C. Lord,   J. Chem. Phys.   26   (1957)   690.

[18]   A. Cabana,   C. Sandorfy,   Spectrochim. Acta   18   (1962)   843.

[19]   E. Castellucci,   J. Mol. Struct.   23   (1974)   449.

[20]   J. Yin,   M. E. Green,   J. Phys. Chem. A   102   (1998)   7181.

[21]   T. Asada,   H. Haraguchi,   K. Kitaura,   J. Phys. Chem. A   105   (2001) 7423.

Figure Captions

Fig. 1.   Structures of the protonated methylamine clusters obtained from DFT calculations at the B3LYP/cc-pVDZ level.   (a) C_1 and (b) C_2 structures of $(CH_3NH_2)_2H^+$, (c) $(CH_3NH_2)_3H^+$, (d) $(CH_3NH_2)_4H^+$.   Nitrogen atoms are denoted by solid circles.   Bond distances indicated are in units of Å.

Fig. 2.   Theoretical infrared spectra of (a) CH_3NH_2 and (b) $CH_3NH_3^+$ obtained from DFT calculations.   The numbers on the ordinates stand for the infrared absorption intensities in units of km mol^{-1}.   Note that the intensities of the bands marked with the asterisk are magnified by a factor of 10 for clear comparison.   (c) Infrared photodissociation spectrum of $(CH_3NH_3)^+$–Ar.

Fig. 3.   (a) Infrared photodissociation spectrum of $(CH_3NH_2)_2H^+$.   Theoretical spectra obtained from DFT calculations by assuming (b) C_2 and (c) C_1 structures for $(CH_3NH_2)_2H^+$. The infrared absorption intensities are in units of km mol^{-1}.

Fig. 4.   Infrared photodissociation spectra of (a) $(CH_3NH_2)_3H^+$ and (c) $(CH_3NH_2)_4H^+$. Theoretical spectra of (b) $(CH_3NH_2)_3H^+$ and (d) $(CH_3NH_2)_4H^+$ obtained from DFT calculations.   The infrared absorption intensities are in units of km mol^{-1}.
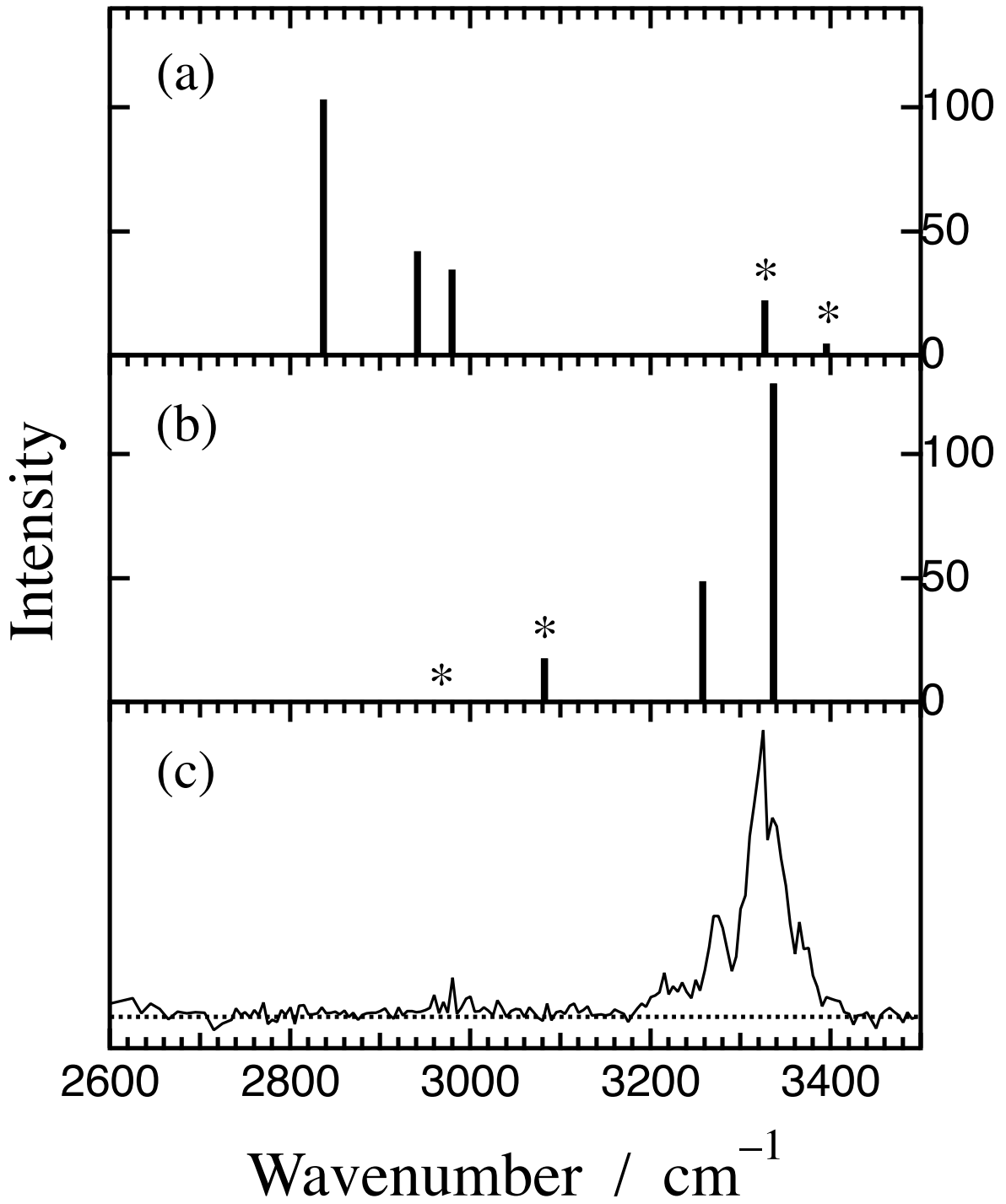
Fig. 2. Michi et al.
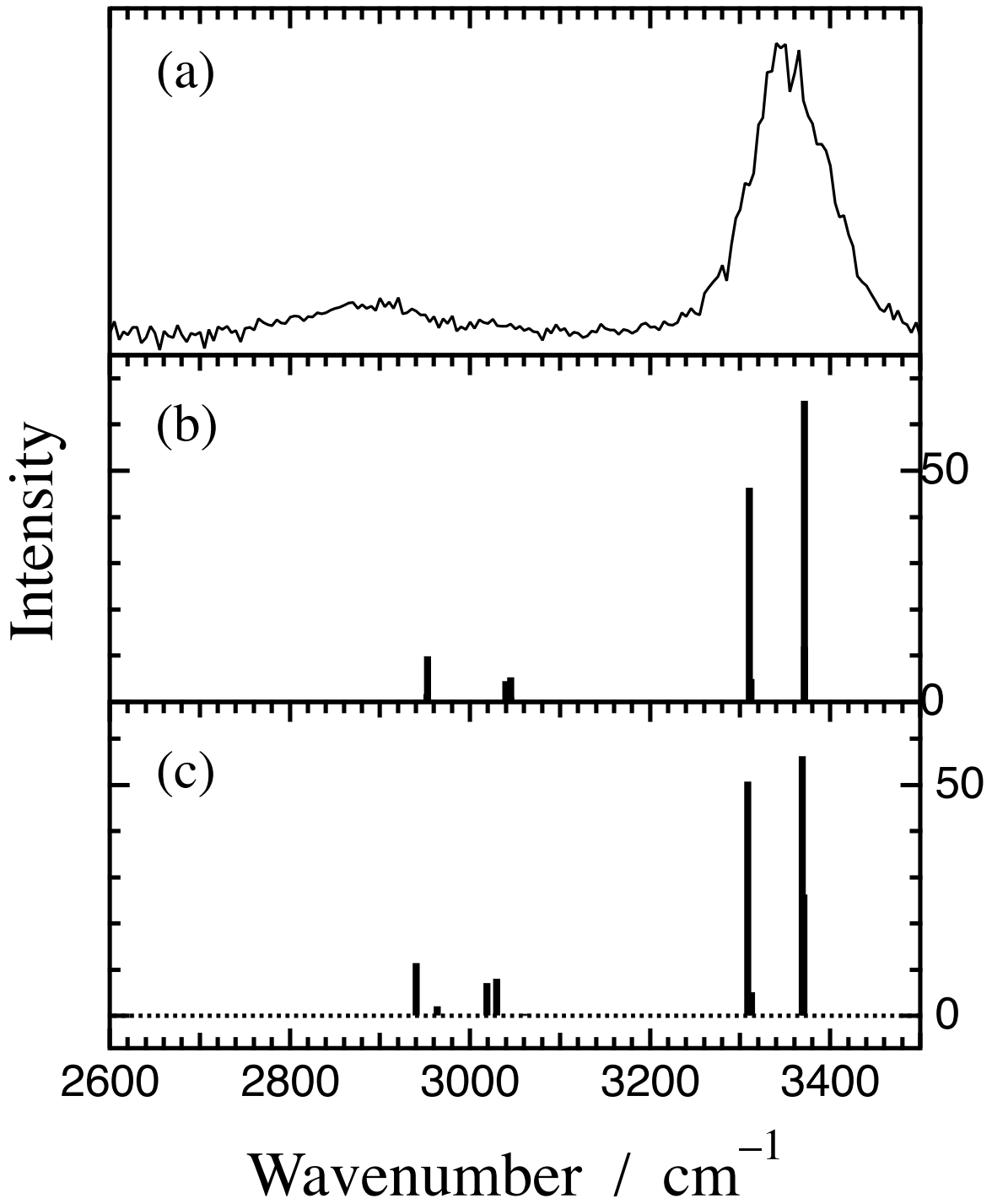
Fig. 3. Michi et al.

Fig. 4. Michi et al.